

## Electron tunneling in a metal-protein-metal junction investigated by scanning tunneling and conductive atomic force spectroscopies

Laura Andolfi, Anna Rita Bizzarri, and Salvatore Cannistraro<sup>a)</sup>

*Biophysics and Nanoscience Centre, CNISM, Facoltà di Scienze, Università della Tuscia, I-01100 Viterbo, Italy*

(Received 28 August 2006; accepted 22 September 2006; published online 3 November 2006)

The electron tunneling across a redox protein covalently bound to Au(111) electrode is investigated by both scanning tunneling and conductive atomic force spectroscopies. Although the current-voltage curves, detected by the two techniques, refer to different tunneling junctions, they are analyzed within the same transport model. By evaluating the electron transmission probability of each element constituting the tunneling junctions, the electron transport properties of the protein macromolecule are singled out. These results represent an advancement in understanding current flow through protein macromolecule in tunneling experiments, also in the perspectives of applications in nanobioelectronics. © 2006 American Institute of Physics.

[DOI: 10.1063/1.2385223]

The use of single protein molecules inserted into hybrid systems has gained progressive interest allowing to combine natural biological functions, such as binding, catalysis, biorecognition, and electron transfer, with processing power of modern microelectronics for the realization of biosensors and nanodevices.<sup>1,2</sup> In view of nanobioelectronic applications, redox metalloproteins are particularly relevant for their inherent capability in transferring single electrons over long distances and in a fast, directional way.<sup>3,4</sup>

Reliable nanobioelectronic devices rely on the formation of stable and robust contacts between single protein and metal electrode to achieve an effective electronic conduction. Essentially, two methods have been applied to investigate the conduction through a single protein chemically bound to a metal electrode: scanning tunneling spectroscopy<sup>4–8</sup> (STS) and conductive atomic force spectroscopy (CAFS).<sup>9,10</sup> In STS, the tip is held stationary on the top of a single protein, forming a gap between the tip and the protein, the tunneling current being used to control vertical tip positioning. Current-voltage (*I-V*) curves, measured as a function of the bias after disengaging the feedback loop, bear information on the tunneling characteristics of both protein and tip-protein gap.<sup>11</sup> Appreciable current signal can be recorded in STS for a wide range of tip-protein vertical distances; this allows acquiring images of proteins with different topologies.<sup>4–10,12</sup>

In CAFS, the tip is directly placed in contact with the single biomolecule at a controlled force and the tunneling current is measured by applying a bias voltage.<sup>11</sup> CAFS has the unique advantage of simultaneously providing topography and current images, thus coupling the conductive properties directly to the morphology of the investigated samples. On the other hand, in CAFS, even if the tip is positioned much closer to the protein than in STS, no tunneling current is measured at very low forces; such an effect may arise from a high contact resistance at low applied force.<sup>8,13</sup> This could also be at the origin of the difficulty to achieve current imaging on protein samples.<sup>9</sup>

STS and CAFS are therefore complementary techniques that can disclose interesting features of the electronic conduction properties of single proteins. The two experimental setups result into different electrode-protein-tip junctions (see Fig. 1). In both cases a chemical contact between protein and Au(111) substrate (e.g., a S–Au covalent bond) is established. In CAFS [see Fig. 1(a)], once the contact resistance between the tip and the protein is overcome, the current tunnels from the tip toward the substrate through the protein, or vice versa depending on the bias polarity. At variance, in STS [see Fig. 1(b)], the tip is away from the protein and the current tunnels from the tip toward the substrate, through both the gap and the protein, or vice versa. This might give rise to discordant results when an analysis of currents detected by the two techniques is performed on the same molecular system.<sup>13</sup>

The aim of the present work is to provide a consistent description of the *I-V* characteristics recorded by both STS and CAFS for a redox protein covalently bound to a gold electrode. In this framework, we have applied a tunneling transport model by taking into account the different elements which contribute to the total electron transmission probability through the junctions.<sup>13–15</sup> Such an approach has been checked on mutant plastocyanin (PCSS), that was genetically engineered to introduce a S–S bridge available for covalent binding to gold.<sup>16</sup>

In CAFS experiments, PCSS anchored to gold was physically contacted with a platinum coated atomic force

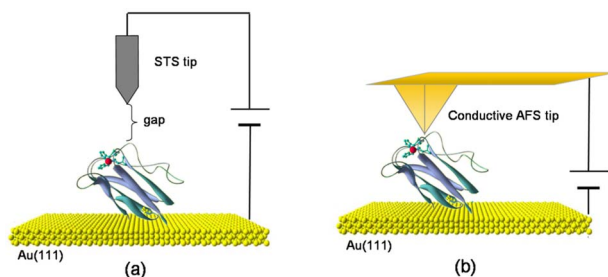


FIG. 1. (Color online) Schematic illustration of the single PCSS molecule as probed by the two experimental setups: STS (a) and CAFS (b).

<sup>a)</sup> Author to whom correspondence should be addressed; electronic mail: cannistr@unitus.it

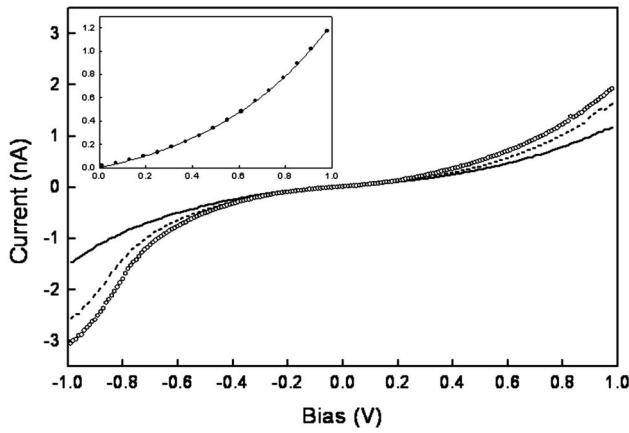


FIG. 2.  $I$ - $V$  curves as measured by CAFS on PCSS anchored on gold at different applied loads: 3 nN (straight line), 4 nN (segment line), and 6 nN (open circle). Inset: fitting curve (straight line) of the experimental  $I$ - $V$  curve (dots) at an applied load of 3 nN. Only one experimental value every four is shown for clarity. Measurements were carried out under dry nitrogen atmosphere to minimize water contamination.

microscopy probe. Figure 2 shows the resulting  $I$ - $V$  curves at moderate applied loads (3–6 nN) at which a good electric contact is established.<sup>9</sup>  $I$ - $V$  curves are almost overlapping in the low bias region ( $\pm 0.2$  V), while progressively higher current intensity values are detected at larger bias when the applied load is increased. At 3 nN, the curve is almost symmetric, while some asymmetry appears at higher loads.

In STS measurements, the tip is positioned on top of a single protein at a distance settled by the engage tunneling current and bias; afterwards the feedback is disabled and  $I$ - $V$  curves are registered. The  $I$ - $V$  curves, shown in Fig. 3, refer to different engage biases; this means that at fixed engage tunneling current the resistance and then the gap between the tip and the protein are widened with increasing the engage bias. A decrement in current intensity is registered as long as higher engage bias is applied and an almost symmetric trend is observed for all curves. It is worth noting that in STS, despite the significant distance between the tip and the protein, an appreciable current signal can be always regis-

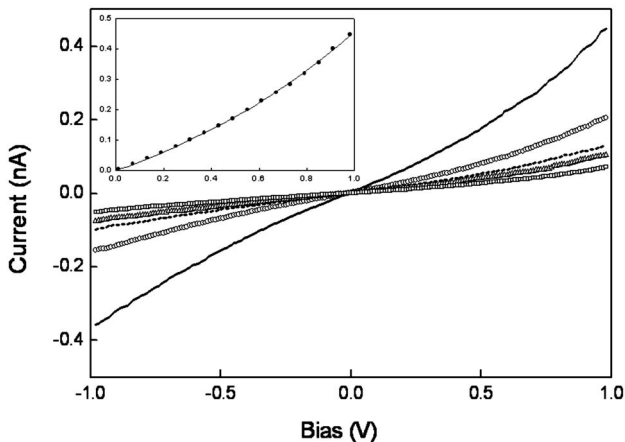


FIG. 3.  $I$ - $V$  curves as obtained by STS on PCSS anchored on gold at tunneling current of 50 pA and increasing engage biases: 0.2 V (open square), 0.4 V (open triangles), 0.6 V (segment line), 0.8 V (open circles), and 1 V (straight line). Inset: fitting curve (straight line) of the experimental  $I$ - $V$  curve (dots) at engage bias of 0.2 V. Only one experimental value every four is shown for clarity. Measurements were carried out under dry nitrogen atmosphere to minimize water contamination.

TABLE I. Barrier height  $\varphi_{\text{mol}}$ , barrier length  $L_{\text{mol}}$ , and decay constant  $\beta_{\text{mol}}$ , as a function of the applied loads, obtained from fitting the  $I$ - $V$  curves measured by CAFS. In all the cases, errors are less than 1%.

Force (nN)	$L_{\text{mol}}$ ( $\text{\AA}$ )	$\varphi_{\text{mol}}$ (eV)	$\beta_{\text{mol}}$ ( $\text{\AA}^{-1}$ )
3.0	15.8	1.93	0.56
4.0	16.4	1.72	0.54
6.0	16.2	1.73	0.54

tered, and the current intensity of the  $I$ - $V$  curves is lower in STS than in CAFS, especially for bias region above  $\pm 0.4$  V, likely due to the presence of the tip-protein gap.

In order to fit the  $I$ - $V$  curves obtained with the two experimental techniques, we have considered that the current, in direct tunneling, can be described by  $I=VG$ , where  $G$  is the conductance given by the Landauer formula<sup>13</sup>

$$G = 2e^2/hT_{\text{tot}}, \quad (1)$$

where  $e$  is the electron charge,  $h$  is the Planck constant, and  $T_{\text{tot}}$  is the total electron transmission probability, from the electrode to the tip, which can be expressed as the product of the transmissions of the different components.<sup>13–15</sup>

In CAFS measurements,  $T_{\text{tot}}$  can be described as  $T_{\text{CAFS}} = T_{\text{SS-Au}}T_{\text{mol}}T_{\text{tip}}$ , where  $T_{\text{SS-Au}}$  represents the protein-electrode chemical bond (SS-Au),  $T_{\text{mol}}$  describes the conduction through molecule milieu (also including a small amount of residual water, strongly bound to the protein), and  $T_{\text{tip}}$  refers to the physical contact between the protein and the electrode. Under the assumption that a good electric contact is attained when a covalent bond is formed between the molecule and the metal junction,  $T_{\text{SS-Au}}$  can be treated as a constant.<sup>13</sup> On the other hand, the evidence that current can be easily recorded at the applied load of 3 nN indicates that a good electric contact between the tip and the molecule is established.<sup>8,9</sup> Accordingly,  $T_{\text{tip}}$  can be treated as a constant, this being also supported by recent results on azurin, a copper protein similar to PCSS.<sup>4,8,9</sup> The electron transport through the molecule can be approximated as a coherent nonresonant tunneling through a rectangular barrier of height  $\varphi_{\text{mol}}$  and length  $L_{\text{mol}}$ ; accordingly, the transmission probability through the molecule is given by  $T_{\text{mol}} = \exp(-\beta_{\text{mol}}L_{\text{mol}})$ , where  $\beta_{\text{mol}}$  is the decay constant reflecting the strength of electronic coupling across the barrier. Within the analyzed bias range,  $\beta_{\text{mol}}$  can be given through the expression<sup>17</sup>

$$\beta_{\text{mol}} = \frac{4\pi}{h} \sqrt{2m^*(\varphi_{\text{mol}} - eV)}, \quad (2)$$

where  $V$  is the applied bias and  $m^*$  is the effective electron mass to take into account that the barrier is replaced by a set of molecular orbitals; according to Refs. 13, 18, and 19,  $m^*$  has been put equal to  $0.16m$  ( $m$  being the electron mass). The results of the fitting of the  $I$ - $V$  curves, through  $I = 2e^2V/hT_{\text{CAFS}}$ , at the different loads are reported in Table I, an example of the fit being shown in the inset of Fig. 2.

The value of  $L_{\text{mol}}$ , obtained at the 3 nN load, is lower than the expected physical height of the protein on the substrate (about 3 nm); actually, the barrier length does not necessarily coincide with the geometrical distance crossed by the electrons.<sup>20</sup> Interestingly, both the  $L_{\text{mol}}$  and  $\varphi_{\text{mol}}$  values are close to those evaluated by CAFS, at comparable loading forces, for a single azurin molecule (11.7  $\text{\AA}$  and 1.1 eV, respectively).<sup>10</sup> The evidence that the  $L_{\text{mol}}$  and  $\varphi_{\text{mol}}$  values

TABLE II. Barrier height  $\varphi_{\text{mol}}$ , barrier length  $L_{\text{gap}}$ , decay constant  $\beta_{\text{gap}}$ , and  $\gamma$  parameter, as a function of the engage biases, obtained from fitting the  $I$ - $V$  curves measured by STS. In all the cases, errors are less than 1%.

Engage bias (V)	$L_{\text{gap}}$ (Å)	$\varphi_{\text{gap}}$ (eV)	$\beta_{\text{gap}}$ (Å <sup>-1</sup> )	$\gamma$
0.2	3.15	9.1	3.08	0.30
0.4	3.45	9.6	3.16	0.31
0.6	3.60	9.8	3.19	0.32
0.8	3.75	9.8	3.19	0.33
1.0	3.90	10.0	3.22	0.33

are similar, at the three different loads, points out that the structural and the conduction properties of the protein remain practically unaffected in the range of the applied loads, in agreement with what is observed for azurin.<sup>8,10</sup> The decay factor  $\beta_{\text{mol}}$  (calculated for  $V=0$ ) is slightly lower than the values found for electron tunneling across metalloproteins in bulk solution (0.8–1.2 Å<sup>-1</sup>);<sup>15</sup> such a discrepancy can be explained by taking into account the different conditions of measurements (geometrical configurations and single molecule regime).

In STS measurements,  $T_{\text{tot}}$  can be expressed as  $T_{\text{STS}} = T_{\text{SS-Au}} T_{\text{mol}} T_{\text{gap}}$ , where  $T_{\text{SS-Au}}$  and  $T_{\text{mol}}$  have the same meaning as in the CAFS analysis, while  $T_{\text{gap}}$  is the transmission probability through the tip-protein gap. To fit the  $I$ - $V$  curves obtained by STS,  $T_{\text{SS-Au}}$  can be again treated as a constant, while for  $T_{\text{mol}}$  we have assumed the same barrier height and length values that come out from the analysis of the CAFS data at the lowest applied force (3 nN). Furthermore,  $T_{\text{gap}}$ , which results from a coherent nonresonant tunneling through a rectangular barrier of height  $\varphi_{\text{gap}}$  and length  $L_{\text{gap}}$ , can be described by  $\exp(-\beta_{\text{gap}} L_{\text{gap}})$ . Accordingly, the following final expression has been used:

$$T_{\text{STS}} = T_{\text{SS-Au}} e^{-L_{\text{mol}}(4\pi/h)\sqrt{2m^*(\varphi_{\text{mol}} - \gamma eV)}} \times e^{-L_{\text{gap}}(4\pi/h)\sqrt{2m(\varphi_{\text{gap}} - (1-\gamma)eV)}}, \quad (3)$$

where  $\gamma$  is an adjustable fitting parameter to take into account for a possible different potential drop over the vacuum gap and the protein molecule, similarly to other theoretical treatments.<sup>21,22</sup> The results of fitting  $I$ - $V$  curves by the  $I = 2e^2 V/h T_{\text{STS}}$  expression, for the different engage biases, are reported in Table II, an example of the fits being shown in the inset of Fig. 3.

First, we note that the values of the barrier height  $\varphi_{\text{gap}}$  and also the decay constant  $\beta_{\text{gap}}$  (calculated for  $V=0$ ) are in a good agreement with those reported in literature for tunneling through a “vacuum” gap.<sup>15</sup> This confirms that the used approach describes well the tunneling current behavior through the protein gap. On the other hand, the barrier length  $L_{\text{gap}}$  is found to be lower than the geometrical tip-protein distances as estimated in a previous analysis for PCSS anchored to gold.<sup>12</sup> From Table II, we note a slight increase of both  $L_{\text{gap}}$  and  $\varphi_{\text{gap}}$ , as far as higher biases are applied, indicative of a small dependence of the protein-gap barrier on applied voltage and protein-gap size, in agreement with what is shown in Ref. 23.

The extracted  $\gamma$  values indicate that a different potential drop takes place in the protein and vacuum gap. The fact that

a larger drop is observed for the gap finds a confirmation with its larger geometrical distance in comparison to that of the protein.

In conclusion, our approach allows us to extract consistent values of the tunneling conduction properties for the PCSS protein from the  $I$ - $V$  curves, as obtained by the two different techniques. The tunneling barrier length, height, and decay factor  $\beta_{\text{mol}}$  of the protein have been evaluated and have been found to be in a good agreement with data in literature. Notably, this theoretical approach, which can be extended to various molecules, provides the possibility to correlate  $I$ - $V$  data from STS and CAFS, thus allowing to obtain more insight into the intrinsic tunneling properties of the single molecule. Moreover, the approach presented, besides being relevant for understanding the conduction of biomolecules covalently bound to a gold electrode, may deserve some interest in optimizing the application of redox proteins in nanodevices.

This work has been partially supported by the FIRB-MIUR Project “Molecular Nanodevices,” the PRIN-MIUR 2004 project, and the Innesco-CNISM 2005 project. One of the authors (L.A.) acknowledges the Research Grant “Rientro dei Cervelli” from MIUR.

<sup>1</sup>I. Willner, Nat. Biotechnol. **19**, 1023 (2001).

<sup>2</sup>N. L. Rosi and C. A. Mirkin, Chem. Rev. (Washington, D.C.) **105**, 1547 (2005).

<sup>3</sup>I. Willner and B. Willner, Trends Biotechnol. **19**, 222 (2001).

<sup>4</sup>B. Bonanni, D. Alliata, L. Andolfi, A. R. Bizzarri, and S. Cannistraro, in *Surface Science Research Developments*, edited by C. P. Norris (Nova Science, New York, 2005), p. 1.

<sup>5</sup>L. Andolfi, G. W. Canters, M. Ph. Verbeet, and S. Cannistraro, Biophys. Chem. **107**, 107 (2004).

<sup>6</sup>Q. Chi, J. Zhang, P. S. Jensen, H. E. M. Christensen, and J. Ulstrup, Faraday Discuss. **131**, 181 (2006).

<sup>7</sup>G. B. Khomutov, L. V. Belovolova, S. P. Gubin, V. V. Khanin, A. Yu Obydenov, A. N. Sergeev-Cherenkov, E. S. Soldatov, and A. S. Trifonov, Bioelectrochemistry **55**, 177 (2002).

<sup>8</sup>J. J. Davis, C. L. Wrathmell, J. Zhao, and J. Fletcher, J. Mol. Recognit. **17**, 167 (2004).

<sup>9</sup>L. Andolfi and S. Cannistraro, Surf. Sci. **598**, 68 (2005).

<sup>10</sup>J. Zhao, J. Davis, M. S. P. Sansom, and A. Hung, J. Am. Chem. Soc. **126**, 5601 (2004).

<sup>11</sup>T. W. Kelly, E. L. Granstrom, and C. D. Friesbie, Adv. Mater. (Weinheim, Ger.) **11**, 261 (1999).

<sup>12</sup>D. Alliata, L. Andolfi, and S. Cannistraro, Ultramicroscopy **101**, 231 (2004).

<sup>13</sup>A. Solomon, D. Cahen, S. Lindsay, J. Tomfohr, V. B. Engelkes, and C. D. Friesbie, Adv. Mater. (Weinheim, Ger.) **15**, 1881 (2003).

<sup>14</sup>L. A. Bumm, J. J. Arnold, T. D. Dunbar, D. L. Allara, and P. S. Weiss, J. Phys. Chem. B **103**, 8122 (1999).

<sup>15</sup>R. E. Holmlin, R. Haag, M. L. Chabinye, R. F. Ismagilov, A. E. Cohen, A. Terfort, M. A. Rampi, and G. M. Whitesides, J. Am. Chem. Soc. **123**, 5075 (2001).

<sup>16</sup>L. Andolfi, S. Cannistraro, G. W. Canters, P. Facci, A. G. Ficca, I. M. C. Van Amsterdam, and M. Ph. Verbeet, Arch. Biochem. Biophys. **399**, 81 (2002).

<sup>17</sup>S. M. Lindsay, J. Chem. Educ. **82**, 727 (2005).

<sup>18</sup>W. Wang, T. Lee, and M. A. Reed, Phys. Rev. B **68**, 035416 (2003).

<sup>19</sup>C. Joachim and M. Magoga, Chem. Phys. **281**, 347 (2002).

<sup>20</sup>M. Yoshitake and S. Yagyu, Surf. Interface Anal. **36**, 106 (2004).

<sup>21</sup>V. Mujica, M. A. Ratner, and A. Nitzan, Chem. Phys. **281**, 147 (2002).

<sup>22</sup>W. Tian, S. Datta, S. Hong, R. Reifenberger, J. I. Henderson, and C. P. Kubiak, J. Chem. Phys. **109**, 2874 (1998).

<sup>23</sup>D. A. Bonnell and B. D. Huey, in *Scanning Probe Microscopy and Spectroscopy*, edited by Dawn A. Bonnell (Wiley, New York, 2001), p. 7.